Supporting Information

Indium Gallium Oxide Alloys: Electronic Structure, Optical Gap, Surface Space Charge and Chemical Trends within Common Cation Semiconductors

Jack E. N. Swallow,[†,‡] Robert Palgrave,[¶] Philip A. E. Murgatroyd,[†] Anna Regoutz,[¶] Michael Lorenz,[§] Anna Hassa,[§] Marius Grundmann,[§] Holger von Wenckstern,[§] Joel B. Varley,[‖] and Tim D. Veal[*,†]

†*Stephenson Institute for Renewable Energy and Department of Physics, University of Liverpool, Liverpool L69 7ZF, U.K.*

‡*Department of Materials, University of Oxford, Parks Road, Oxford OX1 3PH, U.K.*

¶*Department of Chemistry, University College London, 20 Gordon Street, London WC1H 0AJ, U.K.*

§*Felix Bloch Institute for Solid State Physics, Universität Leipzig, Leipzig, Germany*

‖*Lawrence Livermore National Laboratory, Livermore, California 94550, USA*

E-mail: t.veal@liverpool.ac.uk

Core-level analysis

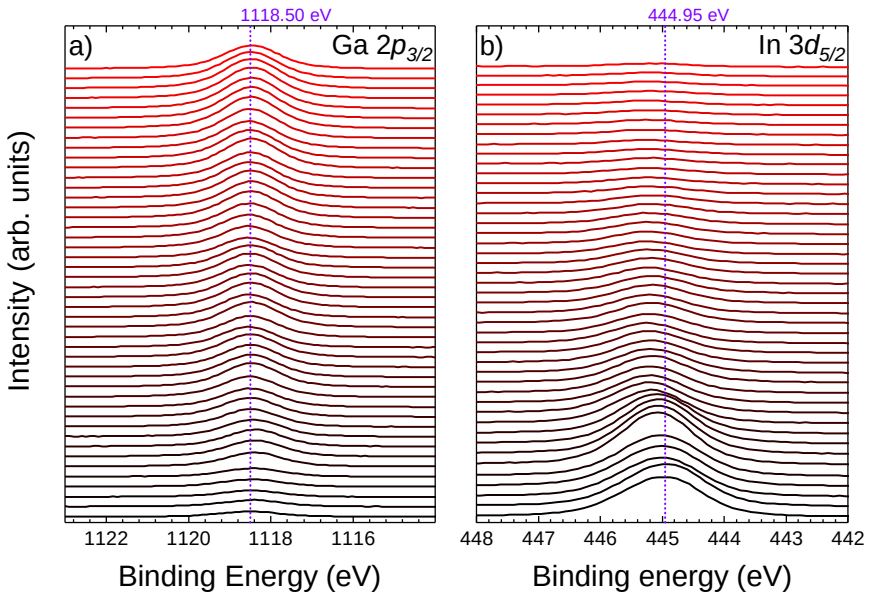

Figure S1: XPS core level spectra of (a) Ga $2p_{3/2}$ and (b) In $3d_{5/2}$ regions of the $(In_xGa_{1-x})_2O_3$ film. 46 spectra were recorded across the film at 1 mm intervals, with the Ga-rich end shown in red at the top of the graphs, with increasing indium content towards the bottom of the graphs in black. Vertical dotted lines are overlaid as a guide for the eye.

Figure S1 shows the Ga $2p$ and In $3d$ core level spectra. The Ga $2p$ peaks slowly diminish in intensity moving down the plot, whilst the In $3d$ intensity grows relatively. This reflects the increasing indium content moving from the Ga-rich side of the film to the In-rich side. Figures S2(a) and (b) display the energy difference between the Ga $2p_{3/2}$ and In $3d_{5/2}$ core level positions and their full width at half maximum (FWHM) as a function of indium content. Peak positions and widths were extracted by fitting single Voigt functions to each core level peak on a Shirley background. In Figure S2(a), the Ga $2p_{3/2}$-In $3d_{5/2}$ energy difference is smaller at lower indium content, increasing slightly until about In(x)$\sim$0.1 before leveling off and remaining relatively flat up until the phase change to bixbyite (at In(x)$\sim$0.7). Here the energy difference rapidly increases which is influenced by a slight increase in binding energy of the Ga $2p_{3/2}$ peak accompanied by a decrease in binding energy of the In $3d_{5/2}$ peak (see Figure S3 for the extracted peak positions of the individual core levels). These trends are reflected in Figure S2(b) where the FWHM of the Ga $2p_{3/2}$ peaks remain relatively

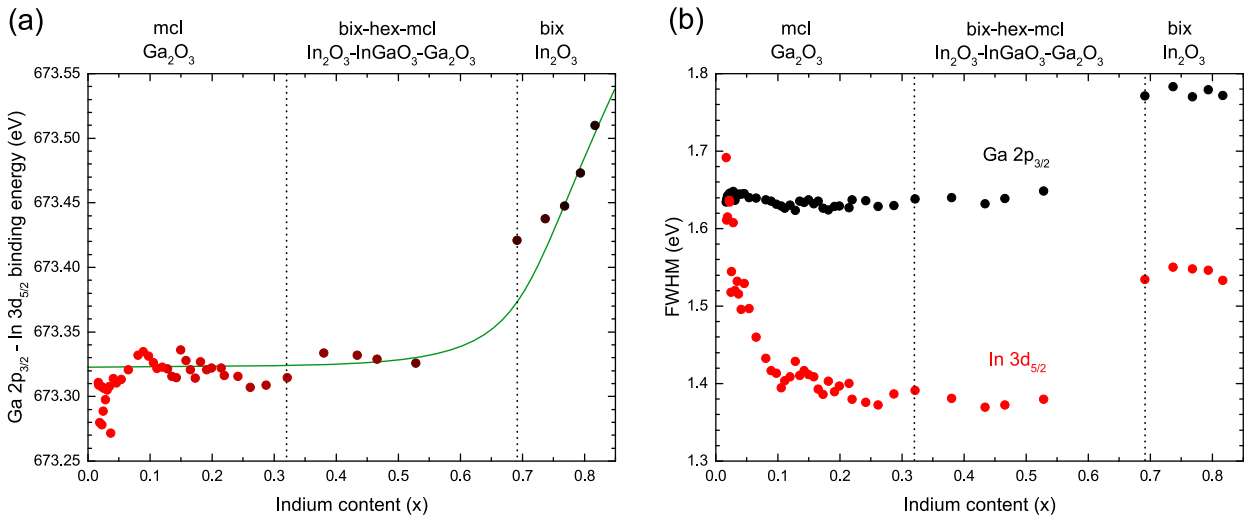

Figure S2: (a) Energy separation between the In $3d_{5/2}$ and Ga $2p_{3/2}$ core levels from XPS as a function of EDX indium content. The line is a guide to the eye. (b) The full width at half maximum (FWHM) of the In $3d_{5/2}$ and Ga $2p_{3/2}$ core levels as a function of EDX indium content. We estimate a moderate uncertainty of around ±0.1 eV on extracted peak positions.

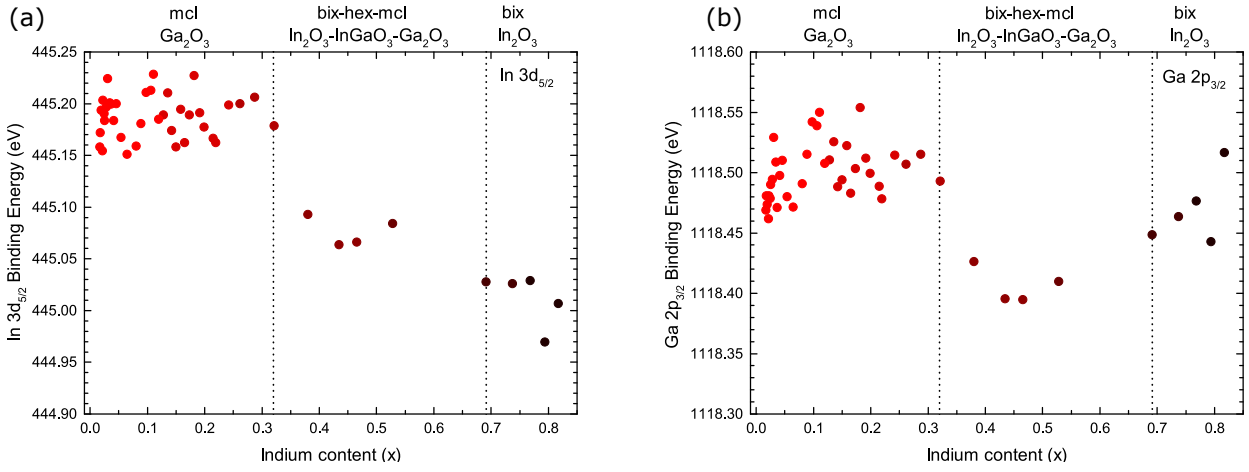

Figure S3: Core level positions relative to E_F as a function of indium content In(x) for (a) In $3d_{5/2}$ and (b) Ga $2p_{3/2}$ core levels. Positions were extracted from the peaks in Figure S1 by fitting Voigt functions to the data with a Shirley background using the CasaXPS software. We estimate a moderate uncertainty of around ±0.1 eV on extracted peak positions.

unaffected until the bixbyite phase change, where they broaden. However, the In $3d_{5/2}$ peak is initially very broad at low In(x) content, before decreasing in FWHM until an indium content of In(x)$\sim$0.1 where it flattens. Indium and gallium have the same oxidation state in $(In_xGa_{1-x})_2O_3$ and similar Pauling electronegativity values of 1.78 and 1.81, respectively. Therefore, the binding energy shifts as a function of alloy composition are expected to be small. This is indeed the case with the separation between Ga $2p_{3/2}$ and In $3d_{5/2}$ peaks only varying by 0.25 eV over the whole composition range and the binding energies with respect to the Fermi level varying over $\sim$0.15 eV for Ga $2p_{3/2}$ and $\sim$0.25 eV for In $3d_{5/2}$. The binding energies of these core levels with respect to the Fermi level fall into three distinct groupings: the highest binding energy ones up to $x = 0.32$ when the structure remains monoclinic; a group of intermediate In $3d_{5/2}$ binding energies and the lowest Ga $2p_{3/2}$ binding energies within the composition region where bixbyite cubic, hexagonal and monoclinic structures all co-exist; and the lowest In $3d_{5/2}$ and intermediate Ga $2p_{3/2}$ binding energies for x above 0.68 where the structure is bixbyite cubic. These discrete changes of binding energy are small, but reflect the different cation coordination in the different structures.

Referring to Figure 1, In preferentially sits on octahedral sites, consistent with previous calculations[1] and expectations from Pauling's ionic radius ratio rule.[2] In all three structures, In can occupy only octahedral sites (6-fold coordinated), with Ga left to occupy the non-octahedral sites - the tetrahedral (4-fold coordinated) or the trigonal (5-fold coordinated) sites in the monoclinic and hexagonal phases. Hence the energy positions depend mainly on the oxygen environment rather than coordination for the In atoms, and because β-Ga_2O_3 has the shortest octahedral O-Ga bond lengths of the three structures, we can rationalize why the In $3d$ would have the highest binding energy in the monoclinic structure, and why the hexagonal phase has the intermediate energy and the bixbyite the smallest. The same holds true for the Ga $2p_{3/2}$, in which case the hexagonal phase is the only one without an octahedral site that Ga can occupy. Therefore it has the lowest binding energies, whilst the other two have octahedral sites that Ga can occupy, giving very similar energies.

Optical Gap

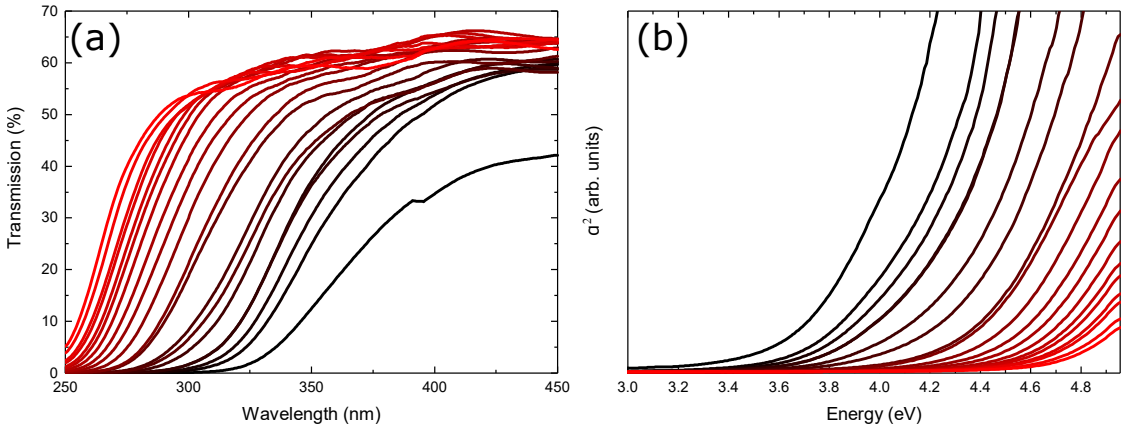

Figure S4: (a) Transmission spectra and (b) associated absorption coefficient squared for the $(In_xGa_{1-x})_2O_3$ film with indium content, x, increasing from red to black.

Figure S4 shows the raw transmission data taken across the composition range of the $(In_xGa_{1-x})_2O_3$ film. The absorption coefficient squared, calculated assuming zero reflection, is also plotted and was used to estimate the optical gaps and band gaps plotted in main manuscript Figures 6 and 7.

Semi-core levels

Figure S5 shows the In4d/Ga 3d semi-core level peaks going from the Ga-rich to In-rich end of the film. A shift in spectral intensity is seen, from the Ga 3d peak around $\sim$ 20.5 eV, to the lower energy In 4d peak at $\sim$ 16.5 eV, in agreement of Figure 9(c) and (d) in the main manuscript. This highlights that the film has solely Ga_2O_3's monoclinic phase for the $0 < x < 0.35$ region, whilst even at the highest In contents, the film still has an appreciable Ga content, in agreement with the EDX measurements.

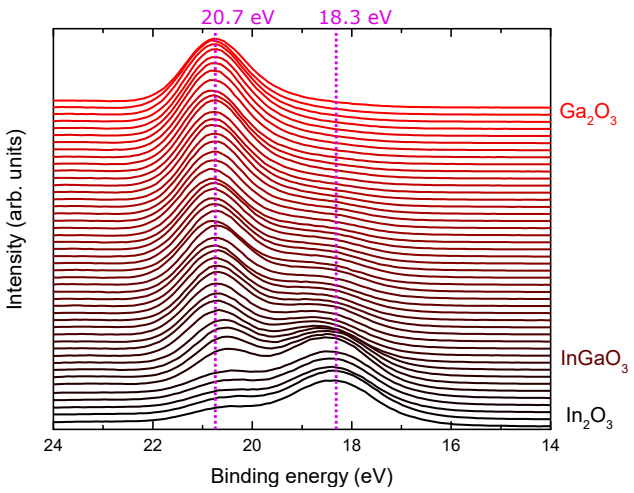

Figure S5: XPS semi-core level spectra of the In 4*d*/Ga 3*d* regions of the $(In_xGa_{1-x})_2O_3$ film. 46 spectra were recorded across the film at 1 mm intervals, with the Ga rich end shown in red at the top of the graph, with increasing indium content towards the bottom of the graph in black. Vertical dotted lines are overlaid as a guide for the eye.

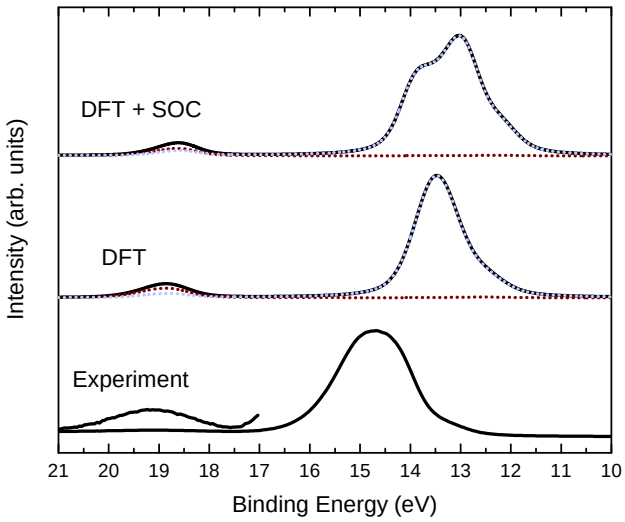

Figure S6: In 4*d* semi-core level spectra of In_2O_3 determined both experimentally, and theoretically using standard DFT and with the inclusion of SOC.

Figure S6 shows the experimental and calculated In 4*d* semi-core level. Calculated spectra are aligned to the VBM of the experimental data. The DFT calculations for In_2O_3 were performed both with and without the inclusion of SOC. Clearly, the energy position of the large In 4*d*-derived peak is not greatly improved upon with the inclusion of SOC when comparing the significantly higher energy experimental peak. However, the shape of this

peak is much closer for the calculation including SOC, which shows more features related to the splitting of the *d*-levels in the calculation. This makes this peak much broader and more irregular in shape, in agreement with experiment. The broadening applied to the DFT is the same as that applied to the valence band spectra in Figure 9(a) of the main manuscript. This may be an underestimate for these levels, as indicated when comparing the experimental data to the theory, where no distinct peaks can be seen in the experiment. However, with further broadening it is clear that the DFT+SOC peak would approach the experiment very quickly. Finally, the O 2*s* derived peak is still clearly not well represented by the DFT approach, being too large in intensity relative to the main In 4*d* peak in both calculations. This issue is known to be related to lower cost theoretical approaches. Greater agreement between theory and experiment has been shown to be obtained for Ga_2O_3 using more expensive theoretical treatments such as GW.[3]

Chemical trends

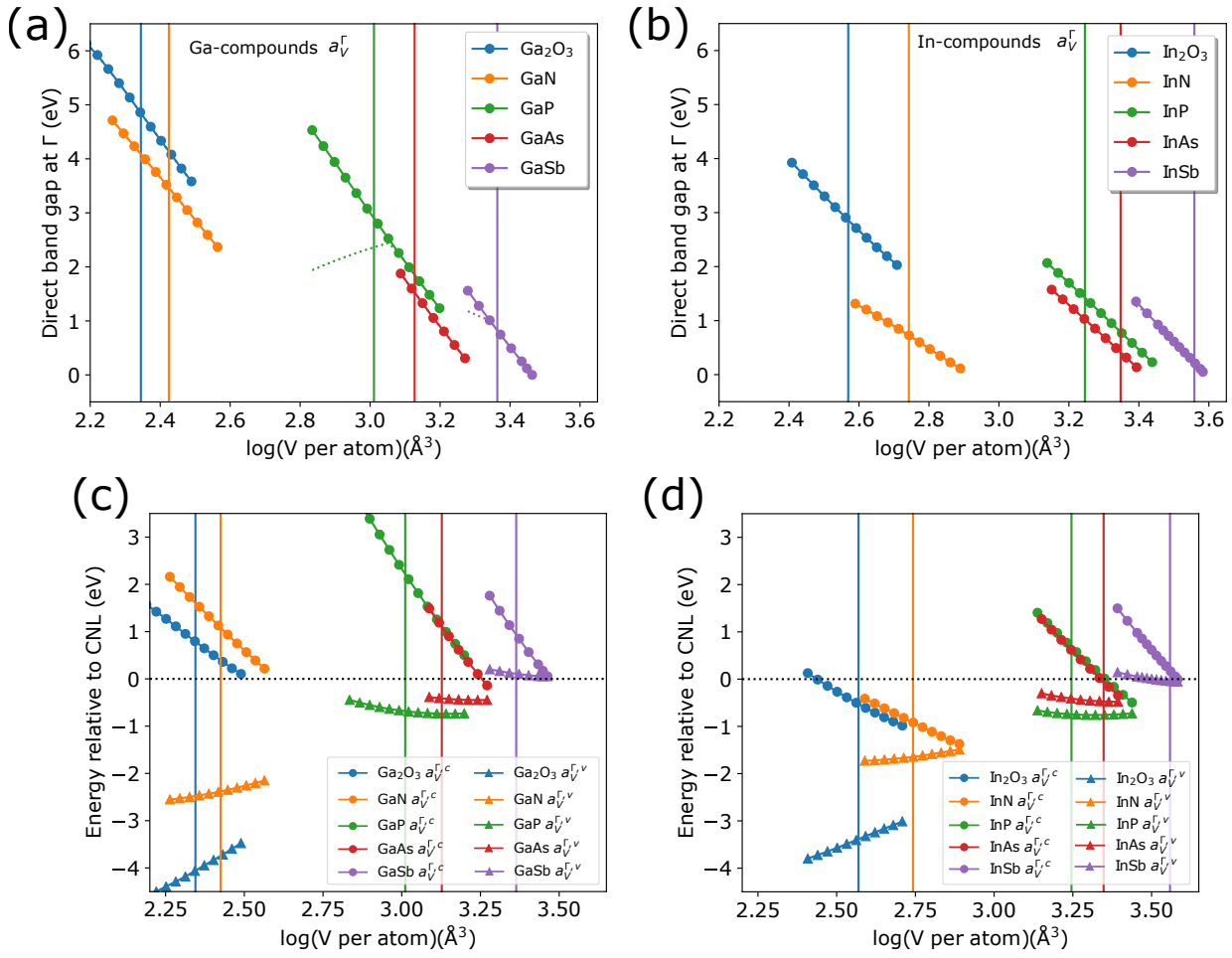

Figure S7: (a)-(b) Calculated band gap deformation potentials for Ga and In-containing compounds for the direct band gaps at the Γ-point. The vertical lines reflect the calculated equilibrium volume per atom. Dashed lines reflect the lower indirect band gaps of the III-V material. (c)-(d) Calculated band gap deformation potentials of the conduction and valence band extrema for Ga and In-containing compounds for the direct band gaps at the Γ-point, as referenced to the branch-point energies. The vertical lines reflect the calculated equilibrium volume per atom and the dashed line at y=0 reflects the charge-neutrality level at which all values are aligned.

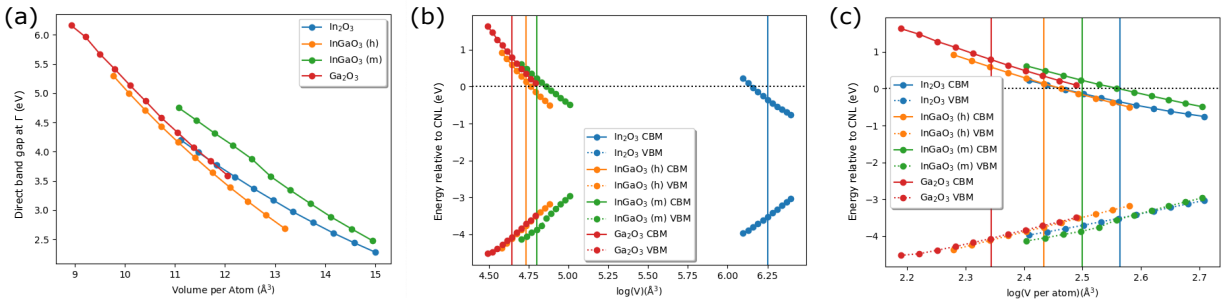

Figure S8: (a) Calculated band gap deformation potentials as a function of unit cell volume per atom for monoclinic Ga_2O_3, bixybite In_2O_3, hexagonal and monoclinic $InGaO_3$ for the direct band gaps at the Γ-point. (b) Calculated band gap deformation potentials of the conduction and valence band extrema as a function of unit cell volume for monoclinic Ga_2O_3, bixybite In_2O_3, hexagonal and monoclinic $InGaO_3$ for the direct band gaps at the Γ-point, as referenced to the charge neutrality level (CNL). (c) Calculated band gap deformation potentials of the conduction and valence band extrema as a function of unit cell volume per atom for monoclinic Ga_2O_3, bixybite In_2O_3, hexagonal and monoclinic $InGaO_3$ for the direct band gaps at the Γ-point, as referenced to the CNL. Note that due to the extremely large unit cell volume of In_2O_3, the equilibrium volume is extremely large relative to the other materials here. The equilibrium volume per atom is much more similar however, due to the large number of atoms per unit cell in In_2O_3.

References

(1) Peelaers, H.; Steiauf, D.; Varley, J. B.; Janotti, A.; Van de Walle, C. G. *Physical Review B* **2015**, *92*, 085206.

(2) Pauling, L. *J. Am. Chem. Soc.* **1929**, *51*, 1010–1026.

(3) Swallow, J. E. N. et al. *Chem. Mater.* **2020**, *32*, 8460–8470.